

Shaping of Multilayer Ceramic Membranes by Dip Coating

J. Luyten,^a J. Cooymans,^a C. Smolders,^a S. Vercauteren,^b E. F. Vansant^b
& R. Leysen^a

^aMaterials Division, VITO, Boeretang 200, B-2400 Mol, Belgium

^bLaboratory of Inorganic Chemistry, Department of Chemistry, University of Antwerp, B-2610 Wilrijk, Belgium

(Received 15 September 1995; revised version received 9 July 1996; accepted 15 July 1996)

Abstract

For the development of new ceramic membranes for gas separative and catalytic membrane reactors, multilayer membranes were synthesized. These membrane configurations consist of three layers: a porous support ($0.1 \mu\text{m} < \text{pore size} < 0.4 \mu\text{m}$), a mesoporous $\gamma\text{-Al}_2\text{O}_3$ interlayer and a gas separative top layer. Different materials for the top layer are being considered.

In this contribution, the characterization of the membranes and the optimization of the manufacturing route for the different material layers are discussed. Some special attention was given to the development of an alternative porous support, adapted from a Reaction Bonded Al_2O_3 (RBAO)-process and to the tailoring of the pore texture of the $\gamma\text{-Al}_2\text{O}_3$ interlayer. Preliminary dip coating experiments proved that the formation of a thin clay or pillared clay layer on an $(\alpha + \gamma)\text{-Al}_2\text{O}_3$ support is possible. © 1996 Elsevier Science Limited.

Des membranes à couches multiples ont été réalisées dans le cadre du développement de nouvelles membranes céramiques pour des réacteurs à séparation gazeuse et à membrane catalytique. Ces types de membranes comprennent trois couches: un support poreux ($0.1 \mu\text{m} < \text{pore} < 0.4 \mu\text{m}$), une couche intermédiaire mésoporeuse en $\gamma\text{-Al}_2\text{O}_3$ et une couche supérieure pour la séparation gazeuse. Différents matériaux sont envisagés pour la couche supérieure.

Ce rapport traite de la caractérisation des membranes et de l'optimisation du mode de fabrication des différents matériaux de couches. Une attention particulière fut accordée au développement d'un nouveau type de support poreux basé sur de l' Al_2O_3 obtenu suivant une adaptation du procédé RBAO (Reaction Bonded Al_2O_3), ainsi qu'à l'adaptation de la texture du pore de la couche intermédiaire en

$\gamma\text{-Al}_2\text{O}_3$. Des expériences préalables de dépôt par immersion ont démontré qu'il est possible de déposer une fine couche d'argile ou d'argile à structure en colonnes sur un substrat en $(\alpha + \gamma)\text{-Al}_2\text{O}_3$.

Introduction

The coupling of a chemical reaction and separation using a membrane, therefore increasing the conversion of equilibrium-limited reactions, opens up new potential application fields for real gas separative membranes. In addition, the use of ceramic membranes makes it also possible to study reactions at temperatures higher than 200°C , which is the working limit for polymeric membranes.

Gas separative and catalytic membrane reactors can improve the conversion of petrochemical reactions such as dehydrogenation, partial oxidation, coupling reactions and deNox reactions.^{1–4} Another application for catalytic ceramic membranes is for the production of hydrogen. Examples are the H_2/CO_2 separation at the end of an integrated coal gasification combined cycle (IGCC) and H_2 winning from the reforming of methane.⁵

To exploit the potentials of inorganic membrane reactors, highly permselective membranes have to be developed. These membranes should also have sufficient permeability, thermal, chemical and mechanical stability.

Recently, significant progress has been made in the crack-free manufacturing of ceramic membranes for gas separation on a lab-scale.^{6,7} Most of the research until now was done on mesoporous membranes, such as $\gamma\text{-Al}_2\text{O}_3$, TiO_2 and ZrO_2 ,^{8–10} but increasingly studies are being performed on microporous, molecular sieving or dense membranes, such as silica, zeolites and Pd–Ag alloys. In contrast to the low permselectivity of

mesoporous membranes, because the mechanism is based on Knudsen diffusion, the new family of membranes permits the realistic separation of different gases. Promising results with microporous ceramic membranes have mostly been obtained with zeolites and silica top layers.¹¹⁻¹³

A multilayer ceramic membrane for gas separation composed of a support material ($0.1 \mu\text{m} < \text{pore size} < 0.4 \mu\text{m}$), a mesoporous membrane layer ($3 \text{ nm} < \text{pore size} < 20 \text{ nm}$) and a gas separative top layer (pore size $< 2 \text{ nm}$) has been developed. The materials studied until now were Al_2O_3 and Reaction Bonded Al_2O_3 (RBAO) for the support and $\gamma\text{-Al}_2\text{O}_3$ for the mesoporous interlayer. For the gas separative top layer different materials are currently being considered, but we describe here the preliminary work on pillared clays.

In this contribution, the optimization of the manufacturing routes for the different material layers produced by conventional powder technology, a special RBAO process route, and the different sol-gel dip coating procedures are discussed. Problems with the conventional support materials (presintered Al_2O_3) are their relative weakness and insufficient surface quality. It is thought that a porous RBAO material, which is much stronger, can solve both problems. The RBAO manufacturing route consists of four steps: (1) mixing (milling) of the Al and Al_2O_3 powders, (2) shaping, (3) oxidation and (4) further heat treatment. An adequate Al particle size and Al distribution, resulting from the milling operation with the Al_2O_3 powder, and a slow heating rate for oxidation are the most important parameters to get a defect-free RBAO structure.

Based on the earlier studies of Burggraaf *et al.*^{14,15} crack free $\gamma\text{-Al}_2\text{O}_3$ mesoporous membranes could be obtained by the addition of polyvinyl alcohol (PVA) to the sol before deposition. The γ to α transformation, which breaks up the fine pore texture of the membrane, can be shifted to higher temperatures by doping with lanthanum.¹⁶ In this way the pore size of the $\gamma\text{-Al}_2\text{O}_3$ layer is optimized.

For the synthesis of the microporous top layer, clay and pillared clays were used. Pillared clays are inorganic microporous materials with a high specific surface. They are prepared by the intercalation of large inorganic species (pillar ions) between the clay sheets, followed by a thermal treatment to convert the pillaring precursor into a rigid oxide pillar (Fig. 1).¹⁷ Pillared clays are multi-functional materials having interesting chemical, catalytic, optical, ionic and electronic properties.^{18,19,24} The challenge is to incorporate this kind of material into a membrane configura-

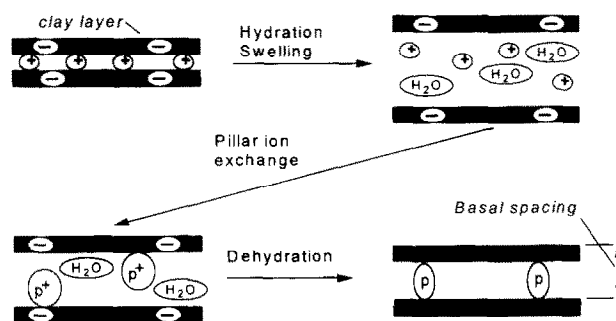


Fig. 1. General scheme for the preparation of a pillared clay.

tion, benefiting from its catalytic and separative properties. Preliminary preparation tests have been performed and the membranes obtained were characterized with scanning electron microscopy (SEM), N_2 -adsorption/desorption and X-ray diffraction (XRD).

Experimental Procedures

Support materials

Discs, pellets and rectangular bars were manufactured by uniaxial pressing and cold isostatic pressing, starting from Al_2O_3 powder (CS400MS, Martinswerk) and from Al/ Al_2O_3 mixtures in a ratio of 2:3 by weight.

The pressing of the powders and the heat treatments of the samples (sintering, oxidation and hot isostatic pressing (HIP)) were controlled so that a porous support with a maximum pore size of about $0.2 \mu\text{m}$ and a pore volume of about 40% was obtained.^{20,21}

After carefully milling, the Al/ Al_2O_3 mixtures were cold pressed with compacting pressures varying between 50 and 200 MPa. After heating slowly, the oxidation temperature was kept constant at 1100°C for 1 h. The sintering was performed between temperatures of 1185 and 1400°C and in some cases followed or replaced by a HIP treatment. The HIP experiments, executed on specimens without encapsulation, were performed at temperatures between 1185 and 1400°C , varying the time (at constant temperature and a pressure of 150 MPa) from 15 min to 2 h. The HIP tests were done under conditions very similar to those described by Holz *et al.*²²

The materials were characterized by thermogravimetric analysis (TGA), mercury porosimetry and four-point bend tests. The thermal shock behaviour of the materials was determined by four-point bend tests of specimens quenched from different temperatures in iced water. The surface quality was checked with scanning electron microscopy and laser profilometer measurements.

Mesoporous interlayer

A boehmite (γ -AlOOH) sol was prepared by hydrolysis of Al-tri-*sec*-butoxide (Janssens Chimica). The sol was peptized with nitric acid. To reduce crack formation during drying and calcination polyvinyl alcohol (PVA) (Merck) was added. For practical reasons, X-ray diffraction (XRD), transmission microscopy (TEM) and N_2 -adsorption/desorption measurements were carried out on unsupported γ -Al₂O₃ layers, assuming that they have a microstructure comparable to the supported layers. This was checked with field emission scanning electron microscopy (FESEM) for the surface pores of supported and unsupported γ -Al₂O₃ layers. The unsupported layers were prepared by drying the sol in Petri dishes at a temperature of 40°C. To study the thermal stability, La-doped samples were made. La(NO₃)₃ solutions of about 3 mol % were directly mixed with the boehmite sol or introduced into the gel by impregnation.¹⁶

Microporous top layer

A sodium exchanged and purified montmorillonite (Bentolite J.B.) and a synthetic clay (Laponite), both provided by Zinchem Benelux, were used to form the top layer. The pillaring precursor ($[Al_{13}O_4(OH)_{24}(H_2O)_{12}]^{7+}$) was prepared by diluting a commercial solution of LOCRO_N L[®] (Hoechst) with HCl.²³ Only the montmorillonite was deposited in its pillared form.

The synthesis procedure of the pillared clay membrane is a variation on the method of Itaya.²⁴ Firstly, a thin clay layer was deposited on the γ -Al₂O₃ surface by dipping a flat support ($(\alpha + \gamma)$ -Al₂O₃) in a clay suspension. The membrane was dried and then soaked for several hours in the pillaring solution so that the sodium ions between the clay sheets were exchanged for the pillar ions. After this ion exchange the membrane was thoroughly washed with water, dried and heated in air at 400°C. Free-standing films on glass plates (for XRD) and flakes (for N_2 -adsorption/desorption) were prepared by a similar procedure.

For the formation of thin clay top layers (with Laponite), the support was just dipped in a clay suspension, followed by a drying and calcination step. The top layers had to be as thin as possible to get a high gas permeation through the membrane.

Results and Discussion

The RBAO manufacturing route consists of four steps: (1) mixing of the Al and Al₂O₃ powders, (2) compaction, (3) oxidation and (4) further heat

treatment. The synthesis of the porous RBAO material requires much care during the manufacturing process. The first and probably the most important step is the milling of the Al/Al₂O₃ powder mixture. The starting powder size of both materials, the Al/Al₂O₃ ratio and the milling time had to be optimized. After the Al/Al₂O₃ milling, Al and Al₂O₃ have to be homogeneously mixed and the Al particles had to be reduced to a critical size. During a slow heating ($\pm 0.5^\circ\text{C}/\text{min}$), the Al₂O₃ skin around the Al particles must continuously break up and reform. In this way, easy access for O₂ for further oxidation of the Al is provided and on the other hand the molten Al stays in place.^{25,26} Otherwise crater-like defects, due to a melt coagulation or sweating of Al above its melting point, are observed.^{20,27,28}

By the correct combination of forming pressure and heat treatment (sintering and/or HIPping), conventional presintered Al₂O₃ and RBAO support materials were manufactured, with a pore size distribution suited for direct sol-gel γ -Al₂O₃ coating. Four-point bend tests showed that the strength of the porous RBAO material was three times higher than that of presintered Al₂O₃.^{20,21} The porous RBAO route used here is a variation on the well-known RBAO process of Claussen (TU. Hamburg).^{26,26,28} The higher strength values (Fig. 2) of this material are due to fine, glass-free Al₂O₃ grains, formed during the oxidation of the Al powder in the mixture. TEM-micrographs (Fig. 3) clearly show the two kinds of Al₂O₃ grains; large primary grains from the original Al₂O₃ and small-grained Al₂O₃ formed during oxidation of the Al fraction.

The thermal shock behaviour of a material can be expressed by:

$$\sigma_{ts} = \psi E \Delta T \alpha / (1 - \nu) \quad (1)$$

σ_{ts} : thermal stress

ψ : stress-reduction factor

E : Young's modulus

ΔT : temperature difference

α : Thermal expansion coefficient

ν : Poisson's ratio

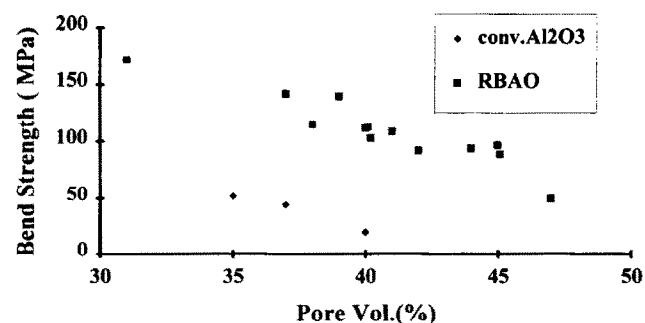


Fig. 2. The mechanical strength (four-point bend) of conventional Al₂O₃ and RBAO series.



Fig. 3. TEM-micrograph of a porous RBAO material showing a bimodal distribution of the Al_2O_3 grain size.

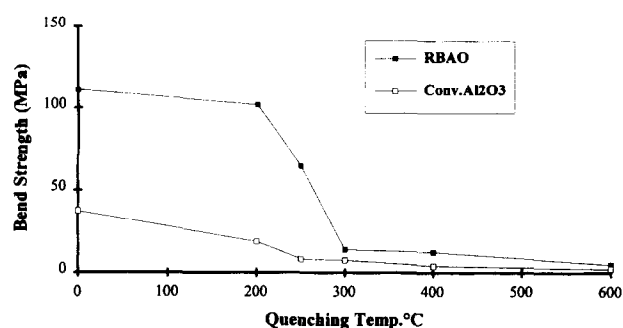


Fig. 4. Thermal shock behaviour of porous RBAO and conventional presintered Al_2O_3 , measured by quenching from different temperatures in ice water.

For most ceramic materials there is a critical temperature (the transition temperature) from which quenching gives a large strength reduction.²⁹

Thermal shock tests demonstrate that the porous RBAO material exhibits the same behaviour and the same transition temperature, as the presintered Al_2O_3 (Fig. 4). Claussen *et al.*²⁸ found that the thermal shock behaviour of dense RBAO and dense Al_2O_3 also followed the same trend.

Although the strength of the RBAO material, after quenching from above the transition temperature, is better than for the conventional Al_2O_3 , further improvement is necessary. A support material with a certain thermo-shock behaviour is necessary for high temperature (> 200°C) membrane applications as envisaged here.

To coat the substrates with a mesoporous $\gamma\text{-Al}_2\text{O}_3$ interlayer, a sol was prepared and a gel layer was formed during the dip coating of the support. The thickness of the gel layer (L_g) equals:³⁰

$$L_g = C/\eta \cdot \sqrt{t} \quad (2)$$

C : a constant combining capillary forces and the permeability of the formed gel.

t : dipping time in seconds.

After gelation, drying and calcination, mesoporous $\gamma\text{-Al}_2\text{O}_3$ membranes are formed. A small

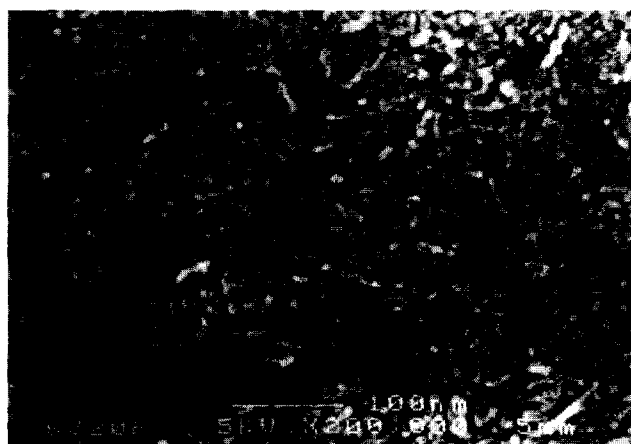


Fig. 5. FESEM micrograph of a top view of a $\gamma\text{-Al}_2\text{O}_3$.

Table 1. Characteristics of $\gamma\text{-Al}_2\text{O}_3$ films after sintering for 30 min at different temperatures

| Sintering temp. (°C) | Specific surface area (m^2/g) | Cylindrical mean pore size (nm) | Porosity (%) | Crystal structure XRD |
|----------------------|---|---------------------------------|--------------|-----------------------|
| 200 | 262 | 2.9 | 41.2 | $\gamma\text{-AlOOH}$ |
| 300 | 265 | 3.1 | 42.8 | $\gamma\text{-AlOOH}$ |
| 400 | 293 | 4.4 | 54.2 | γ |
| 500 | 262 | 4.7 | 53.0 | γ |
| 600 | 216 | 5.4 | 53.0 | γ |
| 700 | 192 | 6.5 | 53.5 | γ |
| 800 | 158 | 7.5 | 52.4 | γ |
| 900 | 137 | 8.0 | 50.4 | γ |
| 1000 | 100 | 9.9 | 47.7 | δ, θ |
| 1200 | 6.7 | 67.8 | 29.5 | α |
| 1400 | 2.7 | 90.2 | 18.1 | α |

amount of polyvinyl alcohol (PVA) is sufficient to prevent crack formation during drying.¹⁵ FESEM micrographs of the surface of supported and unsupported $\gamma\text{-Al}_2\text{O}_3$ films (Fig. 5) indicate no big differences in pore texture between the two kinds of membrane.

Pore size measurements can thus be done on unsupported membranes as was already proposed by Leenaars and Burggraaf.¹⁴ Changes in mean pore size, pore volume, surface area and crystal structure as a function of the temperature are shown in Table 1. According to these results it is clear that the fine pore texture is lost between 900 and 1200°C due to the γ to α phase transformation.³¹ Unsupported $\gamma\text{-Al}_2\text{O}_3$ flakes, with and without La-doping, were heat treated at different temperatures and times. N_2 -adsorption/desorption measurements showed that with La doping the fine pore texture could be stabilized to temperatures of about 1200°C (Fig. 6). Without La doping the fine pore structure was already broken up at temperatures of about 1000°C.

XRD measurements (Table 2) indicate that this was caused by a retardation of the γ to α transformation due to the formation of La oxides on

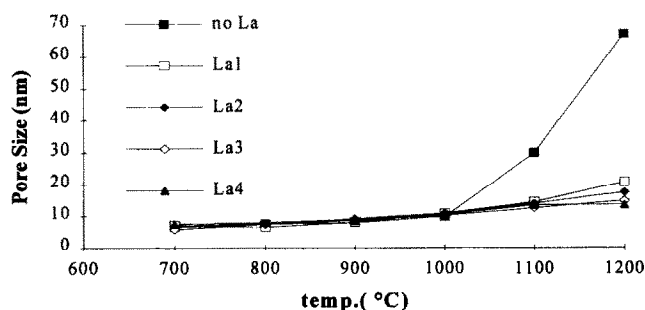


Fig. 6. The influence of La additions on the mean pore size of the γ - Al_2O_3 -membrane after heating for 30 min at different temperatures. Direct mixing with sol, with or without addition of PVA (La1, La2); impregnation of the gel, with or without addition of PVA (La3, La4).

the γ - Al_2O_3 surface. These La oxides retard surface diffusion, and therefore sintering, as well as hampering the α - Al_2O_3 nucleation.¹⁶ Heating for long periods at temperatures up to 1100°C leads to the formation of perovskite structures, such as $\text{LaAl}_{11}\text{O}_{18}$ and LaAlO_3 . Alvarez³² explained the improved thermal stability of the La-doped γ - Al_2O_3 materials by the onset of these perovskite-like phases.

From the results of these experiments it was possible to select heat treatments either with or without La doping in such a way that a γ - Al_2O_3 interlayer can be obtained which is ideally suited for an ultimate support for a microporous top layer.

The pillared clay, or clay, was deposited on a γ - Al_2O_3 membrane (without La) which had been thermally treated at 600°C. Figure 7 shows a SEM picture of such a three-layer system.

XRD results of free-standing pillared clay films indicated that the montmorillonite indeed was pillared, as shown in Fig. 8. Pillared clays normally have a first-order peak in the region $2\theta < 10^\circ$. This (001) reflection corresponds to the basal spacing, which is the distance between two successive clay platelets. A basal spacing of about 18 Å gives immediate indication that pillaring has occurred, since the layer thickness of a montmorillonite is 9.5 Å and the size of the $(\text{Al}_{13}\text{O}_4(\text{OH})_{24}(\text{HO})_{12})^{7+}$ ion is about 9.0 Å.¹⁷ For the free-standing films the basal spacing was about 17.8 Å.

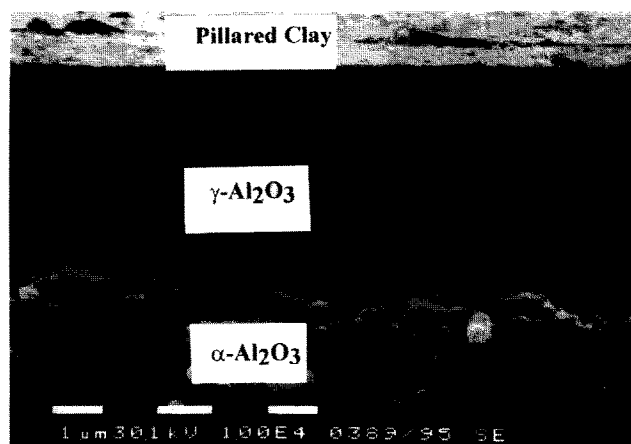


Fig. 7. SEM micrograph, showing a three-layer membrane with a pillared clay top layer.

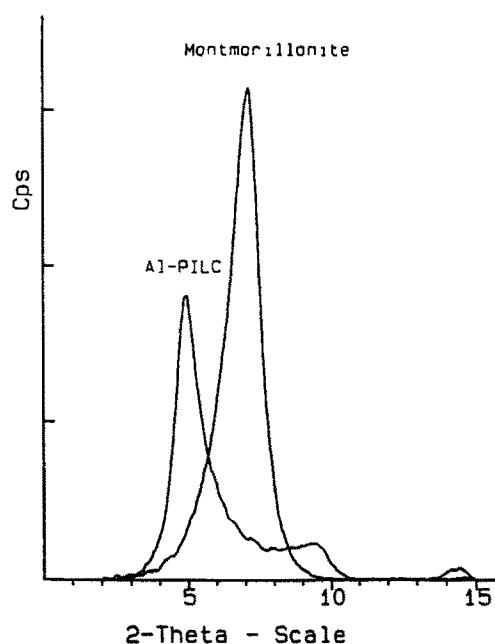


Fig. 8. XRD spectrum of montmorillonite (clay) and alumina-pillared montmorillonite (400°C).

The results of the N_2 -adsorption/desorption measurements of an alumina pillared montmorillonite (=AL-PILC) and a Laponite sample, both calcined at 400°C, are summarized in Table 3. The pore size distributions, calculated with the MP method based on the t-plot, are shown in Figs 9 and 10.

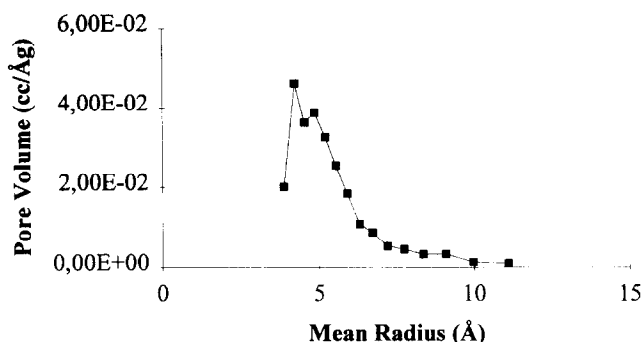
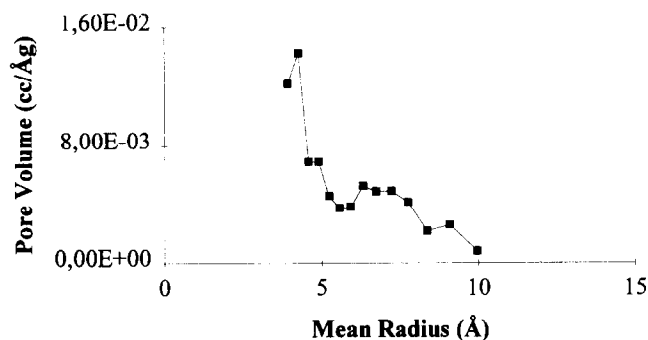
Table 2. Properties of La-doped γ - Al_2O_3 membranes

| Temp. (°C) | Mean pore size (nm) after 30 min | Mean pore size (nm) after 50 h | Crystal structure after 30 min | Crystal structure after 50 h |
|------------|----------------------------------|--------------------------------|--------------------------------|--|
| 800 | 7.6 | 9.9 | γ | $\gamma + \delta$ |
| 900 | 9.3 | 11.7 | $\gamma + \delta$ | $\gamma + \delta$ |
| 1000 | 10.9 | 13.9 | $\gamma + \delta$ | $\gamma + \delta$ |
| 1100 | 14.1 | 18.6 | $\delta + \theta + \gamma$ | $\delta + \theta + \alpha + \gamma' + *$ |
| 1200 | 17.7 | 19.8 | $\theta + \delta + \gamma$ | $\theta + \delta + \alpha + \gamma' + *$ |

*La-Al oxide phases; γ' = shifted γ .

Table 3. Results of N₂-adsorption/desorption measurements of an AL-PILC and a Laponite sample ($T_{\text{calc.}} = 400^{\circ}\text{C}$)

| Materials | S (BET) (m ² /g) | S (Langmuir) (m ² /g) | Micropore volume (cc/g) |
|-----------|----------------------------------|---------------------------------------|----------------------------|
| AL-PILC | 255 | 300 | 0.10 |
| Laponite | 250 | 336 | 0.12 |

**Fig. 9.** Micropore distribution of a Laponite sample.**Fig. 10.** Micropore distribution of an alumina pillared montmorillonite.

The Laponite sample was microporous (type I isotherm) with a mean pore diameter between 0.8 and 1.2 nm. The AL-PILC sample on the contrary contained a reasonable amount of mesopores. Most micropores had a mean diameter of 0.8 nm. This value agrees very well with the interlayer distance (=basal spacing-layer thickness) obtained from the XRD results.

Conclusions

A multilayer membrane for gas separation has been developed. It consists of an alternative RBAO support, a mesoporous $\gamma\text{-Al}_2\text{O}_3$ interlayer and a pillared clay top layer. The new support material, based on a RBAO-process has the advantage of being mechanically stronger than the commonly used presintered Al_2O_3 supports. This allows a reduction of the thickness of the support layer and it even allows a more intense surface treatment (such as polishing and cleaning) to reduce the surface roughness. This kind of sub-

strate was coated with a $\gamma\text{-Al}_2\text{O}_3$ mesoporous interlayer by a sol-gel process. The pore size distribution of this interlayer could be tailored by heat treatment and La doping.

As top layer materials, clay and pillared clays were used. Although the unsupported materials were mainly microporous, gas permeation measurements will be necessary to analyze the complete membrane.

References

1. Saracco, G., Versteeg, G. F. & Van Swaaij, W. P. M., Current hurdles to the success of high-temperature membrane reactors. *J. Membrane Sci.*, **95** (1994) 105–123.
2. Armor, J. N., Challenges in membrane catalysis. *ChemTech* (Sept. 1992) 557–563.
3. Zaman, J. & Chakma, A., Inorganic membrane reactors. *J. Membrane Sci.*, **92** (1994) 1–28.
4. Harold, M. P., Lee, C., Burggraaf, A. J., Keizer, K., Zaspalis, V. T. & de Lange, R. S. A., Catalysis with inorganic membranes. *MRS-Bulletin*, (April 1994) 34–39.
5. Venkataraman, V. K., Rath, L. K. & Stern, S. A., Potential application of microporous inorganic membranes to the separation of industrial gas mixtures. *Key Eng. Mat.*, **61** & **62** (1991) 347–352.
6. Julbe, J., Guizard, C., Larbot, A., Cot, L. & Giroir-Fendler, A., The sol-gel approach to prepare candidate microporous inorganic membranes for membrane reactors. *J. Membrane Sci.*, **77** (1993) 137–153.
7. Burggraaf, A. J. & Keizer, K., *Inorganic Membranes, Synthesis, Characteristics and Applications*, ed. R. R. Bhavé. Van Nostrand Reinhold, New York, 1991, pp. 10–63.
8. Kumar, K. P., Keizer, K., Burggraaf, A. J., Okubo, T. & Nagamoto, H., Textural evolution and phase transformation in titania membranes: part 2 — supported membranes. *J. Mater. Chem.*, **3** (1993) 1151–1159.
9. Xu, Q. & Anderson, M., Sol-gel route to synthesis of microporous ceramic membranes: thermal stability of $\text{TiO}_2\text{-ZrO}_2$ mixed oxides. *J. Am. Ceram. Soc.*, **77** (1994) 1939–1945.
10. Vuren, R. J. V., Bonekamp, B. C., Keizer, K., Uhlhorn, R. J. R., Veringa, H. J. & Burggraaf, A. J., Formation of ceramic alumina membranes for gas separation. In *High Tech Ceramics*, ed. P. Vincenzini. Elsevier Sc. Pub., Amsterdam, 1987, pp. 2235–2245.
11. de Lange, R. S. A., Kumar, K. P., Hekkink, J. H. A., Van de Velde, G. M. H., Keizer, K. & Burggraaf, A. J., Microporous SiO_2 and SiO_2/MO_x ($M = \text{Ti, Zr, Al}$) for ceramic membrane applications; a microstructural study of the sol stage and the consolidated state. *J. Sol-gel Sci. Techn.*, **2** (1994) 489.
12. Bakker, W. J. W., Kapteijn, F., Jansen, K. J., Van Bakkum, H. & Moulijn, J. A., Doorbraak in ontwikkeling zeolietmembranen. *Process Techn.*, **3**(12) (1993) 7.
13. Tsikoyiannis, J. G. & Haag, W. O., Synthesis and characterization of a pure zeolite membrane. *Zeolites*, **12** (1992) 126–130.
14. Leenaars, A. F., Keizer, K. & Burggraaf, A. J., The preparation and characterization of alumina membranes with ultra fine pores. *J. Mat. Sci.*, **19** (1992) 1077–1088.
15. Uhlhorn, R. J. R., Huis in 't Veld, M. H. B. J., Keizer, K. & Burggraaf, A. J., Synthesis of ceramic membranes. Part I. Synthesis of non-supported and supported γ -alumina membranes without defects. *J. Mat. Sci.*, **27** (1992) 527–537.
16. Lin, Y. S. & Burggraaf, A. J., Preparation and characterization of high-temperature thermally stable alumina

- composite membranes. *J. Am. Ceram. Soc.*, **74** (1991) 219–224.
17. Butruille, J. R. & Pinnavaia, T. J., Alumina pillared clays: Methods of preparation and characterization. In *Characterization of Catalytic Materials*, ed. I. Wachs. Butterworth-Heinemann, Boston, 1992, pp. 149–163.
 18. Kleinfeld, E. R. & Ferguson, G. S., Stepwise formation of multilayered nanostructural films from macromolecular precursors. *Science*, **265** (1994) 370–373.
 19. Kikuchi, E. & Matsuda, T., Shape-selective acid catalysis by pillared clays. *Catalysis Today*, **2** (1988) 297–307.
 20. Luyten, J., Coymans, J., Diels, P. & Sleurs, J., RBAO used as part of a membrane configuration. In *Proc. Third Euro-Ceramics*, Sept. 1993, Madrid, Spain, V1, pp. 657–662.
 21. Luyten, J., Coymans, J., Persoons, R., Leysen, R. & Sleurs, J., A new ceramic support material for gas separative membranes and its thermal stability. In *Proc. ICIM3-94*, 10–14 July 1994, Worcester, USA, accepted for publication.
 22. Holz, D., Geerken, M., Wu, S., Janssen, R. & Claussen, N., HIP of Reaction-Bonded Alumina (RBAO) with various ratios of open-to-closed porosity. In *Proc. Hot Isostatic Pressing '93 Congress*, 21–23 April 1993, Antwerp, pp. 425–433.
 23. Molinard, A., Physicochemical and Gas Adsorption Properties of Ion Exchanged Alumina Pillared Clays. PhD thesis, University of Antwerp, Wilrijk, 1994.
 24. Itaya, K., & Bard, A. J., Clay-modified electrodes. 5. Preparation and electrochemical characterization of pillared clay-modified electrodes and membranes. *J. Phys. Chem.*, **89** (1985) 5565–5568.
 25. Wu, S., Holz, D. & Claussen, N., Mechanisms and kinetics of reaction-bonded aluminum oxide ceramics. *J. Amer. Ceram. Soc.*, **76** (1993) 970–980.
 26. Claussen, N., Wu, S. & Holz, D., Reaction bonding of aluminum oxide (RBAO) composites: processing, reaction mechanisms and properties. *J. Eur. Ceram. Soc.*, **14** (1994) 97–109.
 27. Luyten, J., Coymans, J., Diels, P. & Sleurs, J., The effect of powder conditioning on the synthesis of RBAO. *Silicates Industriels*, **7–8** (1992) 91–94.
 28. Claussen, N., Le, T. & Wu, S., Low-shrinkage reaction-bonded alumina. *J. Eur. Ceram. Soc.*, **5** (1989) 29–35.
 29. Davidge, R. W., Thermal stresses and fracture in ceramics. In *Mechanical Behaviour of Ceramics*, Cambridge University Press, Cambridge, 1979, pp. 191–231.
 30. Leenaars, A. F. & Burggraaf, A. J., The preparation and characterization of alumina membranes with ultrafine pores. 2. The formation of supported membranes. *J. Colloid and Interface Sc.*, **105** (1985) 27–40.
 31. Luyten, J. & Sleurs, J., A zeolite- Al_2O_3 membrane configuration. *Silicates Industriels*, **3–4** (1993) 78–80.
 32. Alvarez, L. S., Sanz, J. F., Captain, M. J. & Odriozola, J. A., Onset of perovskite formation in the catalytic system $\text{La}_2\text{O}_3/\gamma\text{-Al}_2\text{O}_3$. *Catalysis Letters*, **21** (1993) 89–97.